Soft Matter

Cite this: *Soft Matter*, 2012, **8**, 4421

www.rsc.org/softmatter

PAPER

Role of pH gradients in the actuation of electro-responsive polyelectrolyte gels†

P. J. Glazer,[ab] M. van Erp,[a] A. Embrechts,[a] S. G. Lemay*[bc] and E. Mendes*[a]

Received 21st December 2011, Accepted 30th January 2012
DOI: 10.1039/c2sm07435d

Polyelectrolyte gels are able to mimic artificial muscles, swelling, shrinking or bending in response to environmental stimuli. Mechanical response is also observed in the presence of an electric field, in which case electrical energy is directly converted into mechanical energy. Although several mechanisms have been proposed to describe electro-actuating in polyelectrolyte gels, no consensus yet exists on which mechanisms are responsible for this phenomenon. Here we use a universal pH indicator to investigate the role of localized pH changes in the gel during bending electro-actuation. We show that, when the gel is not in contact with the electrodes, a pH wave propagating from the electrodes is not the factor that triggers or determines the amplitude of electro-actuation. We also show that, surprisingly, the direction of actuation depends on the salt concentration in the surrounding electrolyte. The polarity of actuation is consistent with models based on dynamic enrichment and depletion of electrolyte for low salt conditions, but reverses at physiological salt concentrations. This suggests that not all experimental observations can be described in terms of a single simple model, and that further theoretical work is needed in the case of physiological salt conditions.

1. Introduction

Polyelectrolyte gels are fascinating physico-chemical systems. Since the discovery in the late seventies by T. Tanaka[1,2] that they can exhibit a discontinuous volume phase transitions by small variations of external parameters such as temperature, solvent quality or pH, the field has attracted a large number of scientists. The ability to produce mechanical work with a water-based soft-matter system placed polyelectrolyte gels at the top of the list of smart materials candidates[3–7] able to mimic muscles.[8,9] More generally, control over swelling, shrinking and bending behaviour of polyelectrolyte gels in response to environmental stimuli enables direct conversion of electrostatic energy into mechanical energy. The characteristic time of response associated with those changes is governed by diffusion of ions and water across the gel and, therefore, it can be significantly reduced when dealing with small dimensions. This fact promoted the use of polyelectrolyte gels in miniaturized actuators such as stimuli-responsive valves[10] or active drug delivery systems.[11,12] Despite recent progress, however, many aspects concerning the physical chemistry of electro-actuation remain unclear. In particular, it is perhaps surprising that there is still no broad consensus on the main mechanisms that drive actuation in electroresponsive gels. Several distinct mechanisms have been proposed (in some cases including quantitative predictions)[2,4,13–18] and, in each case, specific experiments were interpreted as corroborating the mechanism. The variety of interpretations arises without doubt from the complexity of the system, the broad range of concepts involved (chemical equilibrium, polymer physics, osmosis, electroosmosis, electrostatics in electrolytes, electrophoresis, electrochemistry, *etc.*) and the large number of experimental variables (different gels, synthesis protocols, experimental configurations). In particular, we emphasize here that there are three distinct configurations allowing for bending actuation: (i) gel immersed in (salt) solution with both electrodes placed far away from the sample;[9,14,19–21] (ii) gel in solution with both electrodes in contact with the gel surface;[2,8] (iii) gel placed in air with both electrodes touching the sample surface.[4,15–18,22] It is not *a priori* clear that the same mechanism is dominant in each of these different situations.

Before introducing experiments aimed at evaluating the contribution of various mechanisms during actuation, it is convenient to recall them briefly. Consider the case of a rod-shape gel placed in solution between two electrodes (Fig. 1a) that bends under the effect of a transverse electric field, as illustrated in Fig. 1b. The mechanisms proposed in the literature to explain this behavior, illustrated schematically in the historical order in Fig. 1c–f, can be divided into four main categories:

- the Coulomb mechanism (Fig. 1c), in which bending is attributed to the external electric field exerting a net force on

[a]*Chemical Engineering, Delft University of Technology, The Netherlands. E-mail: e.mendes@tudelft.nl*
[b]*Bionanoscience, Delft University of Technology, The Netherlands. E-mail: s.g.lemay@utwente.nl*
[c]*MESA+ Institute for Nanotechnology, University of Twente, The Netherlands*

† Electronic supplementary information (ESI) available. See DOI: 10.1039/c2sm07435d

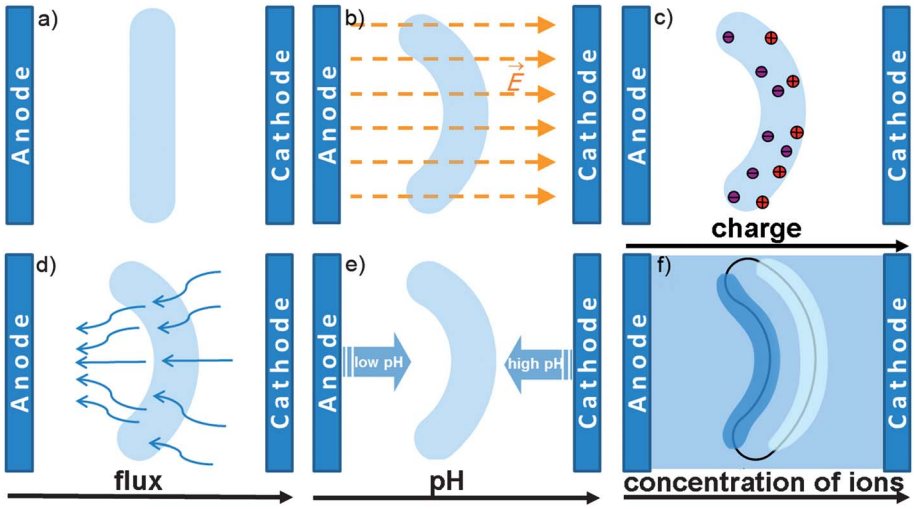

Fig. 1 Actuation of electroresponsive polyelectrolyte gel placed in salt solution and schematic illustration of historically proposed models to explain electroactuation. Rod-like gel (a) before and (b) after applying electric potential. Electroactuation mechanisms (detailed description in the text): (c) Coulomb mechanism, (d) electroosmosis mechanism, (e) electrochemical mechanism, and (f) dynamic enrichment/depletion mechanism (darker and lighter colours at the gel/solution boundaries represent ion accumulation and depletion at the anode and cathode side, respectively).

mobile ions, causing a stationary current inside the gel, as well as on the charged groups attached to the polymer network. As a consequence, the gel is pulled towards one of the electrodes, the anode for the case of an anionic gel studied here.[2,23]

- the electroosmosis mechanism (Fig. 1d), which relates electroactuation to water transport associated with migration of the gel's counterions. It is postulated that anisotropic contraction is governed by an electrophoretic migration of counterions that drags water along and cause the gel to locally contract or swell, leading to bending at larger scales.[4,14]

- the electrochemical mechanism (Fig. 1e), in which actuation is attributed to changes in the gel's protonation state due to local pH changes near the electrodes.[16–18]

- the dynamic enrichment/depletion mechanism (Fig. 1f), which was described by Doi *and co-authors*,[13] attributes electroactuation to the dynamical accumulation (or depletion) of ions on both sides of the gel at the solution interface. Such changes in local ionic strength in turn change local swelling/shrinking near the gel faces, causing bending. This accumulation and depletion of ions of both signs at both interfaces is not a static phenomenon, but is instead a dynamical, non-equilibrium effect caused by asymmetries between cationic and anionic transport inside the gel.

Depending on the nature of the gel, the kind of salt solution used, the sample position in relation to the electrodes and so forth, more than one of these mechanisms can act simultaneously and drive the gel response.[13,24,25]

In this report we will confront experimental results with the two most established mechanisms:[18,21,23,26] the electrochemical mechanism and the dynamic enrichment/depletion mechanism. To fully identify the contribution of each of those two mechanisms involved in electroactuation of polyelectrolyte gels, one would ideally have access to the distribution of ionic species, the water flux and the osmotic pressure gradients in space and time during actuation. As a first step in this direction, we present below a study that makes use of a method based on a universal pH indicator probe to provide quantitative information on the space-temporal distribution of pH during actuation.

2. Materials and methods

Polyacrylamide gels are synthesized by free radical polymerization. Briefly, 4 ml of acrylamide/bis-acrylamide aqueous solution (Sigma Aldrich, A9926) and 20 ml of demineralised and deionised water (MilliQ, resistivity higher than 18 MΩ cm) are mixed together. Ammonium persulfate (10 mg) (Sigma Aldrich, A3678, purity >98%) is added as a radical initiator and *N*,*N*,*N*′,*N*′-tetramethylethylenediamine (20 μl), (Sigma Aldrich, T9281, purity >99.0%) as an accelerator. The solution is then poured into a Teflon mold and left overnight to complete polymerization, yielding a polyacrylamide gel with dimensions 10 cm × 3 cm × 0.3 cm. Demineralised water is placed over the top of the mold in order to reduce oxygen diffusion. The top part of the mold is then removed and the formed gel is placed in a 2 M NaOH solution (Sigma Aldrich, 71689, purity >98.0%) to hydrolyse the amine groups R–NH_2. This process is diffusion limited, so the time needed for complete hydrolysis varies with the gel size. Here the polyacrylamide gels are placed in 2 M NaOH for 2 days.

When the gel is placed in 2 M NaOH solution, conversion of amine groups into ionized carboxylic groups occurs. In a highly ionized polyacrylamide gel, the fraction of the carboxyl groups ionized at any moment is about 20 percent[2,27] Charges on the polymer chains are set by the $–COO^-$ groups and are neutralized inside the gel by Na^+ counterions. The gel is then placed in an excess of demineralised and deionised water, and since the concentration of the free ions inside the gel is not equal to that in the outer solution, a counterion osmotic pressure difference is created. Mobile Na^+ ions tend to decrease the concentration gradient trying to diffuse to the outer solution. However, electroneutrality impeaches them from leaving the gel and the osmotic pressure difference instead pumps water in, causing swelling of the gel. Only a small amount of Na^+ ions can escape to bulk

solution, as determined by the Donnan equilibrium.[28] The time associated with this swelling process is measured in days (see ESI† for more details). As the gel volume increases, the density of ionized groups decreases, therefore also decreasing the osmotic pressure difference. Each time the water is replaced, the gel reaches its final volume as a balance between polymer matrix–solvent affinity, network elasticity, which resists expansion, and charged groups–mobile ions interactions.[29] By repeatedly replacing the water solution, equilibrium is eventually reached and the gel reaches the maximum swelling degree. The gel can take up to 17 times its own weight in water before reaching this equilibrium swelling. Directly before performing electro-actuation experiments, the gel is cut into rectangular beams (7 cm × 0.5 cm × 0.5 cm).

For consistency between the various experiments described here, all gels were allowed to reach swelling equilibrium in demineralised water. Actuation experiments, however, were carried out in aqueous electrolytes containing varying concentrations of salt. In principle a gel has a different equilibrium swelling when placed in a solution with a given salt concentration. Whereas diffusion-driven de-swelling kinetics occur on a time scale of hours, actuation experiments in the presence of electric field are carried out in a matter of minutes, immediately after the gel is placed in salty solution (see ESI† for more details). This separation of time scales insures that the gel is in a similar state for measurements carried out at different salt concentrations.

For the electroactuation measurements, a Flat Bed Electrophoresis Unit MULTI (Carl Roth GMBH) was used. This unit consists of a glass trough with a grid for distance measurements beneath it and two platinum wires mounted in movable frames which served as electrodes. The distance between the electrodes was set to 10 cm, the gel placed mid-way between the electrodes (unless noted otherwise), and an electric potential difference of 15 V applied. Whatever current is necessary to maintain this voltage drop is provided by the power supply. A potential drop of 1.2 V is needed before water hydrolysis can take place.[8] Because the applied potential is much larger than 1.2 V, the variations in the electrolysis potential are relatively small and therefore the electric field is approximately constant in all the experiments. This allows us to compare the influence of salt concentration on gel electroresponsiveness. The potential difference, measured with a Keithley 6517A Electrometer and two Ag|AgCl electrodes located at the centre of the trough and separated by a distance equal to the typical gel sample thickness (~0.5 cm), was 0.5 V.

In experiments where the pH change was visualized, universal pH indicator (Fluka #31282—Universal indicator solution pH 3.0–10.0) was added to 0.1 M KCl solution (1 : 43 ratio). To verify that the marker did not significantly influence the gel responsiveness by changing salt solution parameters, we monitored how the addition of pH indicator to the KCl solution changed the current measured during actuation and found no significant change (see ESI† for more details).

3. Results

While some quantitative information about an average pH value inside the gel can be obtained by direct measurements with electrodes[16] or by theoretical calculations,[30] the distribution of pH inside the gel during actuation is difficult to measure directly on a microscopic level without disrupting the sample integrity. To overcome this difficulty and non-invasively visualize the dynamics of the pH gradient *in situ* during actuation of the gel, we employed a universal pH indicator as a probe. A similar experiment was performed by Bassil *et al.*,[18] in which anthocyanins obtained from red cabbage were used to map pH inside a gel held in air with attached electrodes. Here, unlike the previous study, we concentrated on actuating gels immersed in salt solutions. Because the molecular structure of anthocyanins can easily be destroyed by low or high pH, generating some breakdown products,[31,32] we decided to make use of the universal pH indicator. The indicator allows visualizing the propagation of hydronium and hydroxide ions moving from the electrodes when an electric potential is applied and verifying whether these ions trigger actuation.

The following reactions occur at the electrodes when an electric potential above 1.2 V is applied across Pt electrodes immersed in aqueous solutions:[8]

$$6H_2O_{(l)} \rightarrow O_{2(g)} + 4H_3O^+_{(l)} + 4e^- \text{ (anode)}$$

$$2H_2O_{(l)} + 2e^- \rightarrow H_{2(g)} + 2OH^- \text{ (cathode)}$$

The hydronium and hydroxide ions thus created migrate away from the electrodes and into solution under the influence of the applied electric field. In other words, a pH wave originates from each electrode and propagates with a velocity that is a function of applied voltage. These changes in local pH can cause the chemical equilibrium of the carboxylic groups inside the gel to shift, which can in turn result in anisotropic shrinkage or swelling and cause bending of the gel. This is the electrochemical mechanism illustrated in Fig. 1e.

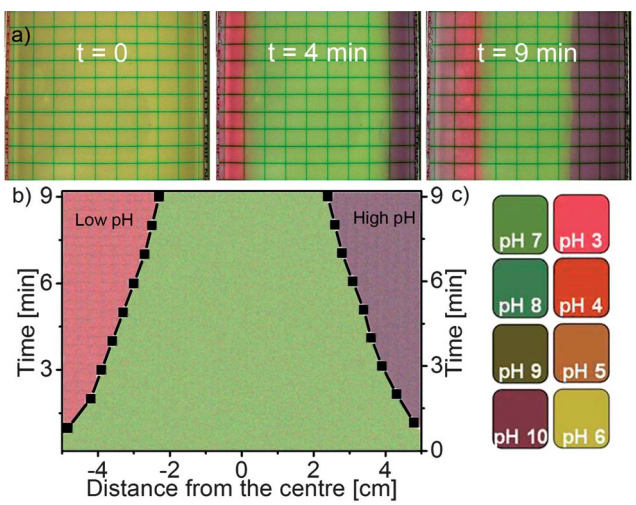

Fig. 2 (a) Images of the immersion tank before applying the electric field (time $t = 0$) and at later times ($t = 4$ and 9 minutes). pH waves originating from the electrodes are clearly observed as colour changes in the vicinity of the electrodes that expand with time. (b) Position of pH propagation front *versus* time. Pink and purple colours represent low pH (<3) and high pH (>10), respectively. (c) Colour scheme associated with the universal pH indicator.

Fig. 2 shows the pH waves and their propagation with time in the absence of gel sample. The colours seen in Fig. 2 correspond directly to the change in local pH values. At the anode (left), water is broken down and H_3O^+ cations are produced. On the cathode (right), OH^- ions are produced. The colours seen in the pictures follow the colour scale provided with the universal indicator used (Fig. 2c). In the vicinity of the anode, the pink colour indicates that the local pH is about 3. Close to the cathode, purple indicates values above 10. In 0.1 M KCl solution, the fronts move with an average speed of about 0.4 cm min^{-1}. The propagation speed is consistent with the electrophoretic mobilities of hydronium and hydroxide ions in water 25 °C (36.3×10^{-4} cm^2 V^{-1} s and 20.5×10^{-4} cm^2 V^{-1} s, respectively[33]). Minor differences between theoretical and experimental values are probably caused by the pH indicator, which acts as a buffer and thus influences ion mobilities.[34] Data points in Fig. 2b indicate the front position with time in relation to the centre of the electrophoresis tank. After nine minutes, hydronium and hydroxide ions are still ~2 cm from the centre of the tank, where the gel is usually located in our actuation experiments. As discussed further below, for a gel placed at the centre of the tank, gel actuation instead starts on a scale of seconds and saturates after 1–2 minutes under similar conditions, suggesting that pH change is not a necessary requirement for actuation.

To further demonstrate that gel electroactuation and pH wave caused by water electrolysis are decoupled phenomena under the present conditions, an experiment with an actuating gel and the pH probe simultaneously present was conducted, as illustrated in Fig. 3. When the electric field is applied, the beam-shaped gels bend significantly over the course of 2 minutes. During that time the pink and purple waves, which indicate the generated pH gradients, move only 0.5 and 0.7 cm away from the electrodes, respectively. No color change is observed in the gel's vicinity. This proves that, when the gel is not touching the electrodes, the development of pH gradients originating from water electrolysis is not necessary for triggering volume changes inside the gel and the corresponding actuation.

The same approach can also be employed when the immersed gel is touching one of the electrodes. For these experiments, the gel is swollen in the presence of the pH indicator such that pH changes deep inside the gel could also be visualized. The results are illustrated in Fig. 4. The darker color of the gel, in comparison to that of the bath solution, indicates that the pH inside the gel is higher than neutral and close to 8. When the gel is in contact with the anode (Fig. 4a), hydronium ions generated at the electrode clearly penetrate into the gel. Conversely, hydroxide ions enter the opposite side of the gel when the cathode is in contact with the opposite side of the gel (Fig. 4b). The pH wave propagating slowly through the gel results in an anisotropic pH distribution. This behavior is analogous to that reported by Bassil *et al.*,[18] except that here the gels are surrounded by electrolyte solution instead of air. It is clear that the electrochemical mechanism can play a role in actuation in our case also. However, the mechanisms involved in actuation when electrodes do not touch the gel (Fig. 3) are simultaneously present here, and the observed behaviour for electrodes touching the gel thus cannot be attributed solely to pH effects.

The time evolution of the pH waves is also plotted in Fig. 4 for both gel positions. An asymmetry exists between the two cases: when touching the anode, the pH wave travels approximately twice as fast (with its position scaling as $\sim t^{1/2}$) compared to the case where the gel touches the cathode (position $\sim t$).

Similar experiments were repeated for non-responsive and responsive gels swollen in pH indicator but placed in the middle of the electrophoresis tank. In the case of a neutral gel, the pH wave does not penetrate the gel structure on the time scale of the experiment (30 minutes). For the responsive gel, on the contrary, the pH wave does penetrate inside once it comes into contact with the gel (see ESI† for more details).

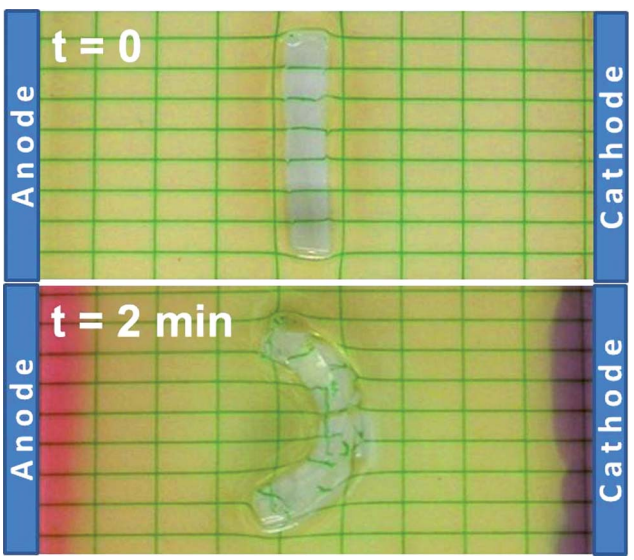

Fig. 3 Gel electroactuation with universal pH indicator added to 0.1 M KCl salt solution. Bending occurs on a timescale faster than that needed for the pH wave originating on the electrodes to achieve the gel. Pink (left) and purple (right) colours represent low and high pH, respectively.

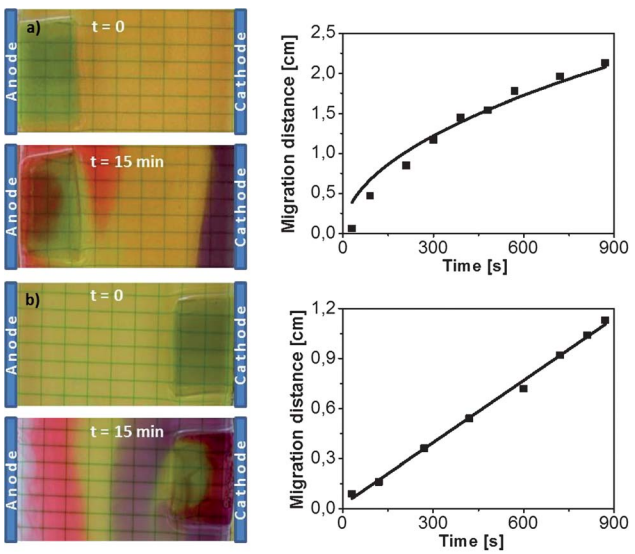

Fig. 4 Evolution of the pH wave for a configuration where the gel touches either (a) the anode, or (b) the cathode, for gels swollen in pH indicator and placed in a 0.1 M KCl solution. Widths of the pH waves from these and intermediate images are also plotted against time for both cases. Solid lines represent fits of the pH propagation distance *versus* time ($\sim t^{1/2}$ and $\sim t$, respectively).

To further explore the factors that determine actuation of polyelectrolyte gels, we measured how the speed of electro-actuation depends on the molarity of the salt solution. This is illustrated in Fig. 5, where the gel curvature (gel bending towards anode) is plotted against time. With increasing salt concentration, the actuation speed also increases until, above 0.3 M KCl, no significant improvement can be achieved by further increase in ionic strength.

In order to obtain significant actuation at low salt concentrations, a stronger driving force is required. To achieve this, the driving voltage was set to 200 V and the electrodes were placed 25 cm apart ($E = 8$ V cm^{-1}). The larger distance ensured that the pH wave from the electrodes did not reach the gel within the timescale of the experiment. An experiment using a bath solution of 10^{-4} M KCl, containing pH indicator, is shown in Fig. 6. Gel actuation occurs but, surprisingly, the bending direction (gel bend towards cathode) is reversed compared to that in experiments at high salt concentration. In addition, a dark region appears around the anode side of the gel, indicating the dynamic creation of a region of low pH. This dark layer grows with time, extending to ~2 mm after 4 min under applied voltage.

4. Discussion

We showed above that, in the case when the immersed gel is not in contact with the electrodes, the electrochemical reactions occurring on the electrodes (Fig. 1e) do not drive electro-actuation: the migration speed of the pH wave was too slow and the bending occurred long before the wave reached the gel. It is therefore interesting to compare our results to the alternative electroactuation mechanisms illustrated in Fig. 1.

The Coulomb mechanism[2,23] (Fig. 1c), which is associated with direct action of the external field on the gel's charges, was not probed directly in our experiments. However, we observe in Fig. 5 that actuation is enhanced at high salt concentrations. This appears qualitatively inconsistent with the Coulomb mechanism, since electrostatic effects are expected to be suppressed at high salt concentrations due to more efficient ionic screening.[35]

The electroosmosis mechanism[4,14] (Fig. 1d) was first introduced to explain the shrinkage of gels in air when electrodes are touching the gel. However, in the experiments reported here, the gel is immersed in salt solution and a reservoir of water and ions of both signs are available around the gel. Any water pumped out of the gel on one side due to electroosmosis can thus be replenished by the corresponding process on the opposite side.

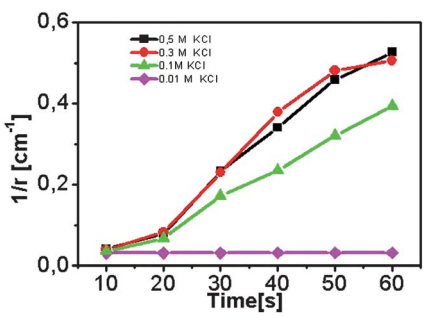

Fig. 5 Gel curvature with time for actuating gel embedded in salt solutions with different KCl concentrations.

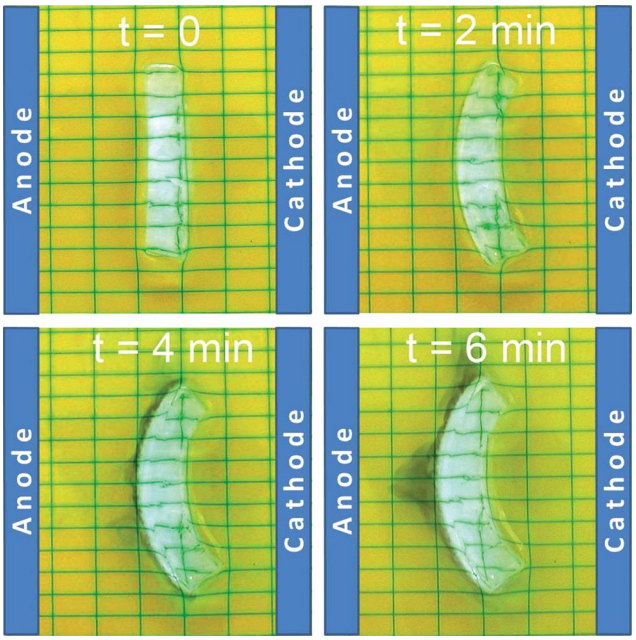

Fig. 6 Visualization of OH^- ion enrichment at the anode side of an electro-actuated polyelectrolyte gel similar to that of Fig. 3, but this time embedded in a low-concentration salt solution (10^{-4} M KCl). The surrounding solution also contains pH indicator. The direction of the electric field is the same as that in Fig. 3, but this time the gel bends towards the opposite side from that observed for high salt concentration (Fig. 3).

Furthermore, electroosmosis is expected to be suppressed at high ionic strength, whereas we observed increases in the degree and speed of actuation at high salt concentrations. For these reasons we rule out the electroosmosis mechanism as the source of actuation in the present configuration.

In what follows, we discuss the dynamic enrichment/depletion mechanism[13,24,33,34] (Fig. 1f) for the cases of low and high salt concentrations separately. Low salt concentrations are defined as KCl concentrations outside the gel that are lower than the concentration of ionised –COOH groups in the gel[13] (around 10^{-3} M). Under these conditions, the equilibrium concentration of mobile cations (mostly Na^+) inside the gel approaches the concentration of ionised –COOH groups in the gel, while the concentration of anions (OH^-) is much lower. This remains true when the gel is taken from its native solution and placed in a KCl solution for actuation experiments. Under these conditions, the dynamic enhancement/depletion mechanism takes a particularly simple form. Inside the gel, the ionic current induced by the external electric field is carried predominantly by cations, since most anions are attached to the gel's chains and cannot move. As a result of this asymmetry inside the gel, a net migration of cations continuously takes place from the side of the gel facing the anode to the side facing the cathode. Simultaneously, anions in the bulk solution outside the gel migrate in the opposite direction, maintaining local charge neutrality. The net effect is a higher concentration of ions (of both signs) on the cathode side. The gel is still electrically neutral, but it is now out of equilibrium: a new swelling equilibrium is found, the gel shrinking due to the extra screening of electrostatic interactions between the charges of the polymer network. A corresponding depletion of

ions takes place on the anode side, leading to swelling of that region. In combination, these changes result in bending of the gel toward the cathode, consistent with experimental observations.

Another feature of the data which follows naturally from the dynamic enrichment/depletion mechanism is the formation of a dark layer on the anode-facing side of the gel (Fig. 6), indicating an increase of pH in this region. Because the gel is anionic, cations (including hydronium ions) are preferentially pumped from the anodic side of the gel and an ion depletion zone with a higher pH is created in this region. To the best of our knowledge, this is the first time such an ion enrichment/depletion layer has been visualized and that its size was obtained experimentally (~2 mm after 4 minutes). Similar ionic depletion and accumulation phenomena have been reported in nanofluidic channels containing asymmetric cation/anion ratios.[36] In the case of nanofluidic channels the charge on the walls of the channel plays the same role as the charges on polymer backbone in polyelectrolyte gel.

For high salt concentrations, the dynamic enrichment/depletion mechanism is more complex. In this case, the equilibrium ionic concentrations inside the gel are in the first approximation equal to those in the surrounding solution.[35] Equilibration starts at the moment when the gel is taken from pure water and placed in the KCl solution, but the equilibration process takes place over several hours. Since this is much longer than the timescale for actuation, the experiments take place far from equilibrium. Solutions of the set of differential equations embodying the dynamic enrichment/depletion mechanism in this scenario have not yet been explored. Potentially, the behaviour observed here, including the reversal of the bending direction at high salt concentration and the absence of the visible enrichment/depletion region in Fig. 3, can be reproduced strictly within the dynamic enrichment/depletion mechanism. However, such an analysis is beyond the scope of the present study.

5. Conclusions

In this paper, we employed a universal pH indicator to investigate the role of localized pH changes originating from water electrolysis during bending electroactuation of hydrolyzed polyacrylamide immersed in salt solution. We demonstrated that, when the gel is not in contact with the electrodes, a pH wave propagating from the electrodes is not the factor that triggers or determines the amplitude of electroactuation.

Our observations are consistent with the dynamic enrichment/depletion mechanism for the case where the gel is immersed in a solution with low salt concentration. In this model, asymmetric flow of ions due to immobile negative charges attached to the gel network causes changes in local salt concentrations in the vicinity of the faces of the gel. The technique of direct visualization of local pH used here allowed us to identify and to measure the dimension of an ion-depletion zone at the anode-facing side of the gel. Such a depletion zone has been theoretically predicted[13] and is a key ingredient in the dynamic enrichment/depletion mechanism. The existence of this depletion zone was experimentally observed here for the first time.

At high salt concentration, the direction of actuation is reversed compared to the low-salt regime. It is not clear whether this behaviour is fully consistent with the dynamic enrichment/depletion. Further theoretical investigations will be required to clarify this issue.

Notes and references

1 T. Tanaka, *Phys. Rev. Lett.*, 1978, **40**, 820–823.
2 T. Tanaka, I. Nishio, S. T. Sun and S. Uenonishio, *Science*, 1982, **218**, 467–469.
3 S. K. Ahn, R. M. Kasi, S. C. Kim, N. Sharma and Y. X. Zhou, *Soft Matter*, 2008, **4**, 1151–1157.
4 J. P. Gong, T. Nitta and Y. Osada, *J. Phys. Chem.*, 1994, **98**, 9583–9587.
5 Y. Osada and J. P. Gong, *Adv. Mater.*, 1998, **10**, 827–837.
6 Y. Osada, J. P. Gong and Y. Tanaka, *J. Macromol. Sci., Part C: Polym. Rev.*, 2004, **44**, 87–112.
7 T. F. Otero, *J. Mater. Chem.*, 2009, **19**, 681–689.
8 H. B. Schreyer, N. Gebhart, K. J. Kim and M. Shahinpoor, *Biomacromolecules*, 2000, **1**, 642–647.
9 H. I. Kim, S. J. Park, S. I. Kim, N. G. Kim and S. J. Kim, *Synth. Met.*, 2005, **155**, 674–676.
10 D. J. Beebe, J. S. Moore, J. M. Bauer, Q. Yu, R. H. Liu, C. Devadoss and B. H. Jo, *Nature*, 2000, **404**, 588–590.
11 K. Sawahata, M. Hara, H. Yasunaga and Y. Osada, *J. Controlled Release*, 1990, **14**, 253–262.
12 P. Bawa, V. Pillay, Y. E. Choonara and L. C. du Toit, *Biomed. Mater.*, 2009, **4**, 022001.
13 M. Doi, M. Matsumoto and Y. Hirose, *Macromolecules*, 1992, **25**, 5504–5511.
14 R. Kishi and Y. Osada, *J. Chem. Soc., Faraday Trans. 1*, 1989, **85**, 655–662.
15 R. Kishi, M. Hasebe, M. Hara and Y. Osada, *Polym. Adv. Technol.*, 1990, **1**, 19–25.
16 Y. Hirose, G. Giannetti, J. Marquardt and T. Tanaka, *J. Phys. Soc. Jpn.*, 1992, **61**, 4085–4097.
17 M. Bassil, J. Davenas and M. El Tahchi, *Sens. Actuators, B*, 2008, **134**, 496–501.
18 M. Bassil, M. El Tahchi, E. Souaid, J. Davenas, G. Azzi and R. Nabbout, *Smart Mater. Struct.*, 2008, **17**, 055017.
19 F. Cherblanc, J. Boscus and J. C. Benet, *C. R. Mec.*, 2008, **336**, 782–787.
20 E. Jabbari, J. Tavakoli and A. S. Sarvestani, *Smart Mater. Struct.*, 2007, **16**, 1614–1620.
21 J. M. Lin, Q. W. Tang, D. Hu, X. M. Sun, Q. H. Li and J. H. Wu, *Colloids Surf., A*, 2009, **346**, 177–183.
22 T. Budtova, I. Suleimenov and S. Frenkel, *Polym. Gels Networks*, 1995, **3**, 387–393.
23 M. Bassil, M. Ibrahim and M. El Tahchi, *Soft Matter*, 2011, **7**, 4833–4838.
24 T. Yamaue, H. Mukai, K. Asaka and M. Doi, *Macromolecules*, 2005, **38**, 1349–1356.
25 S. K. De, N. R. Aluru, B. Johnson, W. C. Crone, D. J. Beebe and J. Moore, *J. Microelectromech. Syst.*, 2002, **11**, 544–555.
26 A. P. Safronov, M. Shakhnovich, A. Kalganov, I. A. Kamalov, T. F. Shklyar, F. A. Blyakhman and G. H. Pollack, *Polymer*, 2011, **52**, 2430–2436.
27 W. M. Leung, D. E. Axelson and D. Syme, *Colloid Polym. Sci.*, 1985, **263**, 812–817.
28 S. L. Cooper, C. H. Bamford and T. Tsuruta,*Polymer Biomaterials in Solution, as Interfaces and as Solids—Festschrift Honoring the 60th Birthday of Dr Allan S. Hoffman*, V.S.P. Intl Science, March 1995.
29 P. Flory, *Principles of Polymer Chemistry*, Cornell University Press, Ithaca, NY, 1953.
30 A. Horta, M. J. Molina, M. R. Gomez-Anton and I. F. Pierola, *J. Phys. Chem. B*, 2008, **112**, 10123–10129.
31 G. H. Laleh, H. Frydoonfar, R. Heidary, R. Jameei and S. Zare, *Pak. J. Nutr.*, 2006, **5**, 90–92.
32 G. J. McDougall, S. Fyffe, P. Dobson and D. Stewart, *Phytochemistry*, 2007, **68**, 1285–1294.
33 A. B. Duso and D. D. Y. Chen, *Anal. Chem.*, 2002, **74**, 2938–2942.
34 A. Persat, M. E. Suss and J. G. Santiago, *Lab Chip*, 2009, **9**, 2454–2469.
35 A. Fernandez-Nieves, A. Fernandez-Barbero and F. J. de las Nieves, *J. Chem. Phys.*, 2001, **115**, 7644–7649.
36 L. J. Cheng and L. J. Guo, *Chem. Soc. Rev.*, 2010, **39**, 923–938.

